J Mater Sci (2007) 42:320–327
DOI 10.1007/s10853-006-1020-9

Synthesis and characterization of silicalite powders and membranes with micro–meso bimodal pores

C. A. Cooper · Y. S. Lin

Received: 15 July 2004 / Accepted: 23 September 2005 / Published online: 8 December 2006

Abstract Silicalite sols containing silicalite agglomerates of 150–380 nm in size were synthesized by hydrothermal synthesis for 0.5–3 days. Silicalite powders and supported silicalite membranes containing micro-meso bimodal pores were prepared by the sol–gel method using these silicalite sols. The silicalite powders contain intracrystalline zeolitic pores (0.54 nm) and intercrystalline mesopores of about 3–4 nm in diameter. For the silicalite powders the mesopore size decreases and mesopore surface area increases with increasing silicalite agglomerate size as a result of a change of the shape of silicalite agglomerates from round to more faceted one. Continuous silicalite thin films of thicknesses ranging from 3 μm to 12 μm were made on α-alumina by the sol–gel dip-coating method. The supported silicalite membranes also contain both zeolitic pores and mesoporous intercrystalline pores. The single gas He permeance of the 3 μm thick α-alumina supported silicalite membrane was found to be from 2.7×10^{-6} to 3.3×10^{-6} mol/m^2 s Pa. These bimodal pore zeolite powders offer the potential as catalysts and sorbents with improved efficiency. The bimodal pore zeolite membrane can be used as support for zeolite and other membranes and as compact packed-bed reactor for chemical reaction.

C. A. Cooper · Y. S. Lin
Department of Chemical and Materials Engineering, University of Cincinnati, Cincinnati, OH 45221-012, USA

Y. S. Lin (✉)
Department of Chemical Engineering, Arizona State University, Tempe, AZ 85267, USA
e-mail: jerry.lin@asu.edu

Introduction

Zeolites have found widespread use in industry as catalysts and adsorbents [1]. Zeolites used in industrial processes are usually in the form of a pellet consisting of micron-sized zeolite crystals bound together on an inorganic support (such as alumina) [2]. These zeolite pellets contain intercrystalline macropores and microporous zeolitic pores. Zeolite powders made of nano or submicron sized zeolite crystallites may find applications as catalysts, adsorbents, and chromatographic packing with improved efficiency. Such micron-sized zeolite powders contain microporous zeolitic pores and mesoporous intercrystalline pores defined by compact nano or submicron sized zeolite crystallites. They offer reduced mass transfer resistance and enhanced zeolite content when used directly as the chromatographic packing materials or as the main constitute in zeolite pellets for large industrial processes.

Zeolite membranes with meso–micro bimodal pores may also be found in many applications. Perhaps the best known use of bimodal pore zeolite membranes is as the seed layer for secondary growth to form a continuous microporous zeolite membrane [3–5]. In this method a layer of zeolite seed crystals is deposited on a support and then, by hydrothermal synthesis, the crystals already in place are grown to the point where all or most intercrystalline gaps are filled. MFI type zeolite membranes, made primarily by the secondary growth method, have shown success in separating xylenes [6] and hydrogen from C_1 to C_4 hydrocarbons [5]. Meso–micropore bimodal zeolite thin films have also received much attention for use as sensors [7, 8], and as supports for supported liquid membranes and for biological membranes. It was recently demon-

strated that mesoporous silica membranes, with a modified hydrophobic surface, could be used to support a liquid ion exchange group for copper ion removal [9]. The liquid ion exchange group in this work is adhered to the surface of a support by way of van der Waals forces only. It is possible that the hydrophobic nature of some zeolites (such as silicalite) could be used in a similar manner to help stabilize a liquid membrane through hydrophobic interactions. Furthermore, the bimodal membranes may be used as a compact but yet efficient packed-bed reactor for reaction and separation applications.

Much work has been done in the past decade on synthesis of zeolite membranes especially of MFI type zeolite [4]. Most work was focused on synthesis of continuous zeolite membranes without mesopores and study of their properties for gas and liquid separation, even in those studies involving preparation of zeolite films with mesopores [3, 5, 6, 10, 11]. The present study was directed towards sol–gel synthesis and characterization of bimodal pore silicalite powder and membranes consisting of zeolitic micropores and intercrystallite mesopores, with emphasis on understudying the effects of crystallite size and shape on zeolite mesopore structure. Silicalite particles and supported membranes consisting of nano or submicron sized silicalite agglomerates were prepared by the sol–gel method. The samples were then characterized using XRD, nitrogen permporisometry, scanning electron microscopy, and gas permeation. The objective of this paper is to report the characteristics and properties of the bimodal pore zeolite powder and membranes prepared in this work.

Experimental

Silicalite powder and membranes were made from a silicalite sol that was prepared using the following method. 0.7 g of NaOH (99.99%, Aldrich) was stirred into 50 ml of tetrapropyl ammonium hydroxide (TPAOH, Aldrich). The solution was contained in a capped 100 ml Teflon flask. The solution was heated to 80 °C and 10 g of fumed silica (Cabot Corporation, Cab-O-Sil M-5, 99.8%) was added slowly. When working with fumed silica a special respirator was used to avoid inhaling the silica particles. After all the fumed silica was added the solution was stirred until it was clear. The solution was then removed from heat and allowed to age for 3 h. The solution was then placed in a Teflon lined autoclave. The autoclave was then sealed and put in an oven at 120 °C. The hydrothermal treatment was run for either 0.5, 1, 2, or 3 days. After the allotted time, the autoclave was removed from the oven and allowed to reach room temperature. The silicalite particles were then removed by centrifuge at 14,000 rpm for 10 min. The silicalite particles were then washed with DI water and centrifuged again. This was done a total of 3 times or until the pH of the silicalite suspension obtained was approximately 10. The particles were washed until a pH of 10 was obtained because this was found to be the most stable. Stable silicalite sol was obtained containing from 10 wt% to 50 wt% silicalite.

Unsupported silicalite films were obtained by drying some of the silicalite sol in petri-dish for 2 days at 40 °C. The films were then ground for 10 min with a quartz mortar and pestle to give silicalite powders. Finally the silicalite powders were calcined at 650 °C for 8 h with a heating rate of 20 °C per hour. The powders were then analyzed by XRD, SEM, and nitrogen porisometry.

The silicalite membranes were prepared on α-alumina supports by dip-coating the silicalite sol described above. The α-alumina supports were prepared by press-sintering of alumina powder (A16, from Alcoa). The discs obtained from this were approximately 20 mm in diameter and 2 mm in thickness. Before dip-coating, the supports were polished using a Metaserv 2000 grinder/polisher from Buehler. The non-support side of the membrane was polished with 500 grit polishing paper only. The support side of the membrane was polished with 500, 800, and then 1200 grit polishing paper. The supports were then washed with deionized water and dried for 2 days at 40 °C. The supports were dried to assure no water content so that the dip coating process would work well. To prepare the silicalite sol for dip-coating, first 0.5 g of hydroxypropyl cellulose (HPC, MW = 100,000) was stirred at room temperature into 100 ml of deionized water. Then the solution was heated to 50 °C and maintained for 2 h. Typically 1–2 wt% silicalite sols were prepared. One gram of the 10 wt% silicalite sol described earlier and 3 g of the HPC solution were diluted with 6 g of deionized water. Then enough 1 M HNO_3 was added to bring the pH to 3–4 (typically 3 drops). After the silicalite dip-coating sol was made the α-alumina supports were dip-coated for 5 s in an Envirco benchtop clean room. The supported membranes were dried and calcined under the same conditions as for the silicalite powders described above.

The crystal structures of the synthesized zeolites were examined by X-ray diffraction (XRD, Siemens D-50, with CuKα_1 radiation, λ = 1.5405 Å). Nitrogen porisometry experiments were run on an ASAP 2010 Micromeretics porosimeter. Nitrogen porisometry was

done on the different silicalite powders with two different modes of operation for mesopores (2–50 nm average pore size) and micropores (below 2 nm). The micropore mode used a molecular pump and measured nitrogen adsorption isotherm down to 10^{-6} relative pressure. However, there is a noticeable difference in the volume of gas adsorbed between the isotherms obtained in the mesopore and micropore modes. This is because the micropore mode uses the molecular pump, which allows the sample to reach a lower equilibrium pressure. Both the mesoporous and microporous software programs were used to evaluate the isotherms obtained.

The surface morphology and cross-section of the membranes were examined using a Hitachi SEM (S-4000). The silica distribution for the α-alumina supported silicalite membrane was examined using energy dispersive spectrometry (EDS, S-4000 Hitachi) with line scanning along the cross section of the membranes. Some membranes were subjected to single gas He permeation as described in a previous publication [12].

Results and discussion

Silicalite powders prepared by grinding the unsupported silicalite films contain particles of about 5–20 μm in size. The size of the particles in the powder depended on how the film was ground. The particles consist of silicalite agglomerates (or aggregates). Figure 1 shows some SEM pictures of the silicalite agglomerates in the powders made by hydrothermal treatment for 0.5, 1, 2, and 3 days, respectively at 120 °C. From visual inspection the average diameters of the silicalite agglomerates were 150, 220, 300, and 380 nm for the 0.5, 1, 2, and 3 days, respectively. As expected, in general the average agglomerate diameter increased with hydrothermal reaction time for all of the silicalite particles synthesized. Table 1 shows the experimentally determined average silicalite particle size from various preparation techniques. All of these samples seen in Table 1 were prepared by standard hydrothermal synthesis techniques, except for the samples with a TEOS silica source, which were made from the steaming of surfactant protected precursors [15].

A general trend that can be seen in Table 1 is that as the reaction temperature and time are increased the agglomerate size is increased. In order to produce small crystals using the hydrothermal synthesis method, a low temperature and long reaction time are needed. Decreasing the temperature increases the rate of nucleation while increasing the temperature increases the rate of crystallization. The average particle size of the silicalite agglomerates obtained in this work corresponds well to what is found in other work, regardless of silica source.

Figure 2 shows the XRD results of calcined and uncalcined silicalite powders that were grown using hydrothermal synthesis for either 1 or 2 days. After the silicalite powders were made most were calcined at 650 °C for 8 h and some were left uncalcined. The 1- and 2-day uncalcined samples have similar XRD peaks which are characteristic for Silicalite and the 1- and 2-day calcined samples have similar XRD peaks

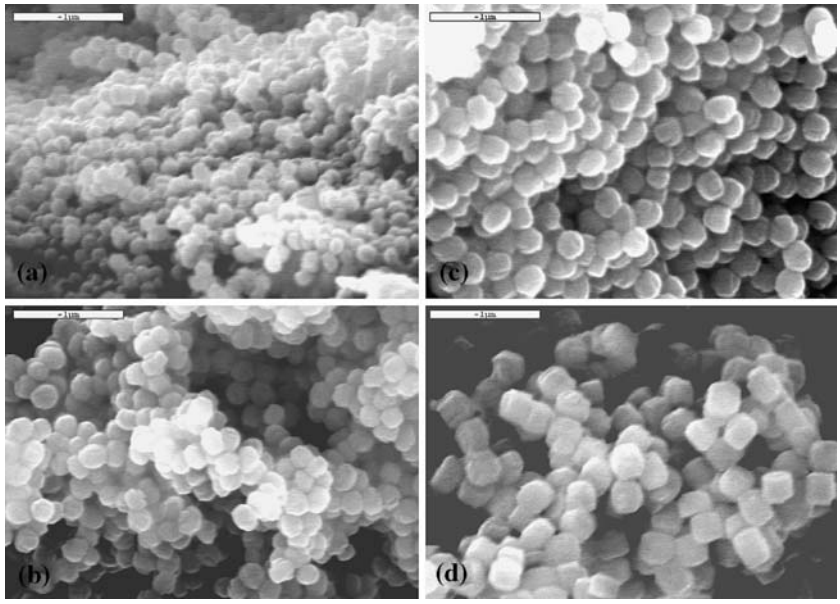

Fig. 1 SEM photographs of silicalite particles grown hydrothermally for (**a**) 0.5 days, (**b**) 1 day, (**c**) 2 days, and (**d**) 3 days at 120 °C. The scale bar is 1 μm for all pictures

Table 1 Comparison of silicalite agglomerate size from different preparation techniques

Silica source	Temperature (°C)	Time (days)	Reference	Particle size (nm)
Sodium silicate	160–180	2	[13]	2,000–5,000
Colloidal silica	160–180	2	[13]	1,000–30,000
TEOS	60	21	[14]	50
TEOS	110–150	1–1.5	[15]	30
TEOS	180	0.5	[16]	100
Fumed silica	185	0.167	[12]	400
Fumed silica	120	3	[17, 18]	200–400
Fumed silica	120	0.5	This work	150
Fumed silica	120	1	This work	220
Fumed silica	120	2	This work	300
Fumed silica	120	3	This work	380

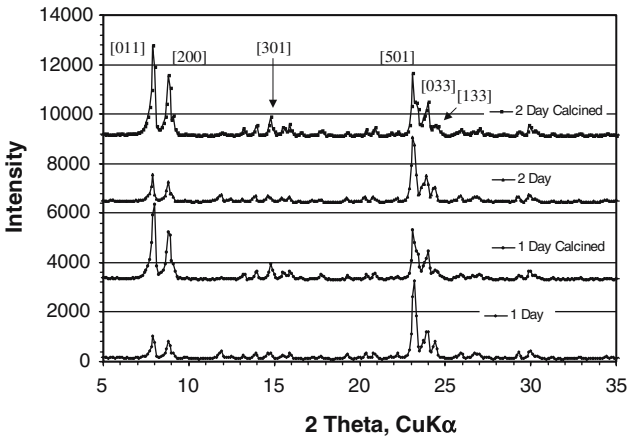

Fig. 2 XRD of calcined and uncalcined silicalite powders made from hydrothermal synthesis lasting 1 or 2 days

which are also characteristic for silicalite. However, there is a noticeable difference between the calcined and uncalcined samples. After calcination the peaks corresponding to [h,k,l] values of 011, 200, and 301 are much more pronounced. The [501], [033], and [133] peaks seem to be less affected by calcination. Similar effects of calcination can be seen elsewhere [5, 14].

For both the 1- and 2-day samples, the intensity of all the major peaks increased after calcination except for the [501] and [133] peaks which decreased. The calcined XRD response is different because of the removal of the TPAOH template by calcination. The intensity of the peaks of the 2-day calcined sample was approximately 20% larger than those of the 1-day calcined sample. The major difference between the 1- and 2-day particles is that the 1-day particles have an average particle size of approximately 220 nm while the 2-day particles have an average particle size of 300 nm. While the d-spacing values, which characterize the microstructure, are characteristic for silicalite, it is apparent that the macrostructure of the zeolite particles is affecting the peak intensity.

Figure 3 shows nitrogen adsorption isotherms for the silicalite powder grown for 0.5 days using the microporous and mesoporous characterization programs. The nitrogen adsorption isotherm in Fig. 3 cannot be characterized by the known isotherm type because the sample contains micropores and mesopores. The section at relative pressures lower than 0.2 has the characteristics of type I isotherms and is used to calculate the micropore size distribution (by the Horvath–Kawazoe method). Adsorption and desorption isotherms obtained by the mesopore mode exhibit hysteresis, characteristic of mesopores. The mesopore size distribution was calculated from the desorption isotherm by the BJH model. The mesopore program gives the total surface area of 429 m^2/g for the 0.5-day silicalite, 359 m^2/g from the silicalite micropores and 70 m^2/g from the intercrystalline pores within the silicalite particles.

Figure 4 shows the average pore diameter for the 0.5-day silicalite powder versus the differential pore volume. Since there is no method developed to successfully handle materials that have both micropores and mesopores, the approach that was used in this work could provide some useful information about the pore structure of the silicalite powders with micro- and mesopores [15]. From Fig. 4 it can be seen that the calculated average pore diameter for the micropores is 5.4 Å. The structure of silicalite is known to contain

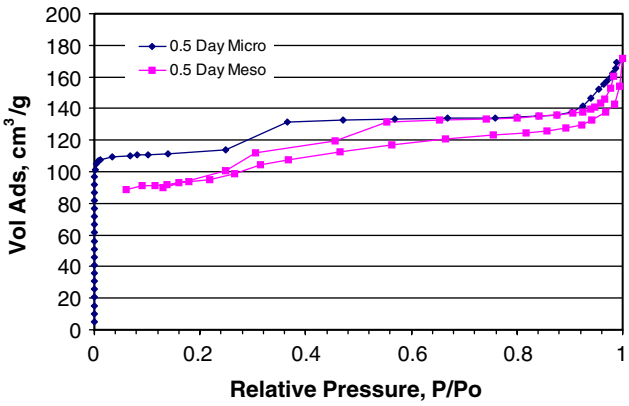

Fig. 3 Characteristic nitrogen adsorption isotherms for silicalite adsorbent grown for 0.5 days using the microporous and mesoporous programs

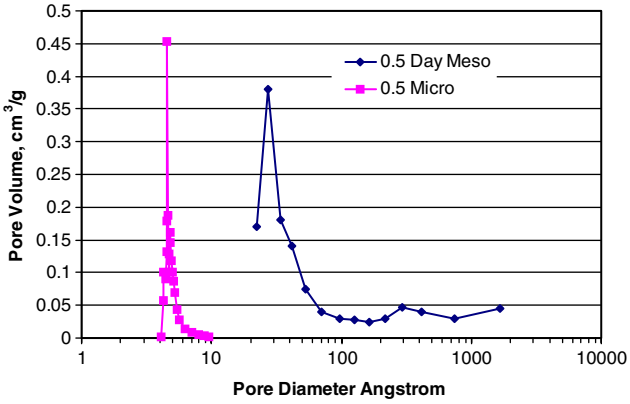

Fig. 4 Average pore diameter for silicalite adsorbent grown for 0.5 days using the microporous and mesoporous programs

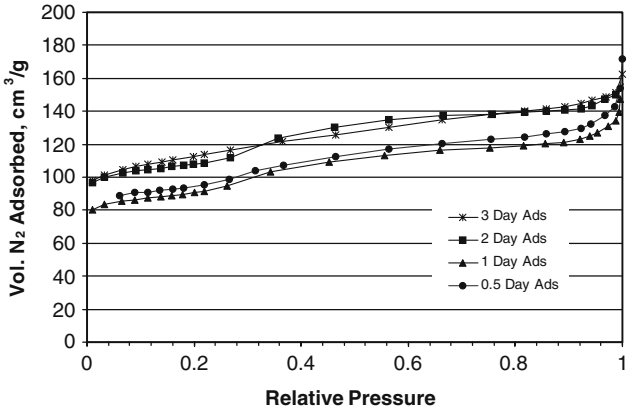

Fig. 5 Adsorption isotherms for silicalite particles grown for 0.5, 1, 2, and 3 days

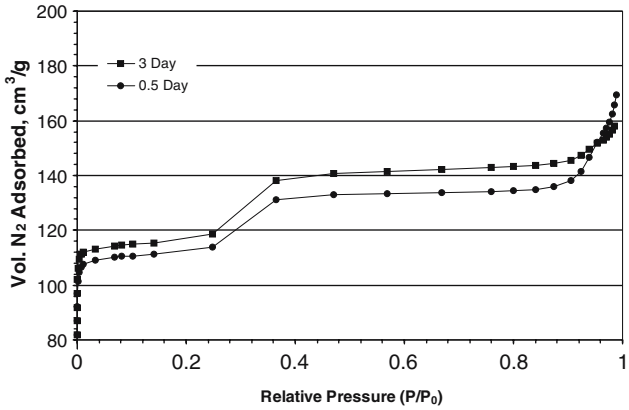

Fig. 6 Low pressure adsorption isotherms for silicalite particles grown for 0.5 and 3 days using a log scale for microporous comparison

zig–zag channels with pores in the A direction with a diameter of 5.4 ± 0.2 Å. Silicalite also contains straight pores in the B direction with an elliptical cross section with dimensions of 5.7 by 5.1 Å. The pore size calculated by the H–K method is close to what would be expected for intracrystalline pores of silicalite.

The average pore diameter in the mesopores range, as calculated from the BJH model, is 4.8 nm. These pores are attributed to spaces created in between the primary zeolite crystals within the silicalite aggregates (150–380 nm). This would indicate that the primary zeolite crystals making the silicalite agglomerates up are on the order of 20–40 nm [15]. From Fig. 4 it can be seen that there are also some larger pores around 30 nm. These pores can be attributed to spaces created in between the aggregates of zeolite crystals. The silicalite agglomerates for the sample are about 150 nm in size. The small intercrystalline pore size indicates these silicalite agglomerates are densely packed with small intercrystalline space.

Figure 5 shows the nitrogen adsorption isotherms for the silicalite powders grown for various periods of time obtained by mesopore mode. The same step increase at a relative pressure of 0.3 is seen for all of the isotherms. The desorption isotherms are not shown, but all show the same general trend as the one seen in Fig. 3. All the isotherms have the same trend and generally increase in volume of N_2 adsorbed with increase in particle growth time. Figure 6 shows the adsorption isotherms for the particles grown for various periods of time obtained by using the micropore mode. The 1- and 2-day data have been omitted for clarity since they have the same general trend and are in between the 0.5 and 3 days. The low pressure region of this graph is characteristic for Type I isotherms. The data in the low pressure range (below 0.2 P/P_0) was nearly identical for all the samples. This makes sense because the silicalite structure is constant in all the samples as verified by XRD. The data at $P/P_0 = 0.3$ (corresponding to pore sizes approximately from 2 nm to 4 nm) is also similar. This seems to suggest that the primary silicalite crystals are close to the same size for the different reaction times. In the area of $P/P_0 = 0.9$ there are major differences between the 0.5- and 3-day samples. This is most likely because the 0.5-day particles are smaller and there is a smaller pore size between the agglomerates.

Table 2 shows how the time of zeolite growth affected the average mesopore structure of the silicalite powders. The mesoporous pore size tends to decrease with increasing growth time. This is the opposite of what would be expected if the particles where perfectly spherical. Since the longer the silicalite agglomerates grow, the larger they become, it would be expected that the intercrystalline pore size would increase. It is possible that a densification process in

Table 2 Affect of zeolite growth time on the mesopore structure of silicalite powders

Silicalite growth (days)	BJH des. pore dia (Å)	BET surf. area (m^2/g)	Mesoporous surf. area (m^2/g)
0.5	36.3	429.2	70.0
1	34.2	435.4	100.9
2	27.0	436.3	120.0
3	26.7	455.4	131.5

the agglomerates accompanies the zeolite growth. However, Fig. 1 shows the shape of silicalite agglomerates changes from round, and elliptical, to square faces as synthesis time increases. There seem to be more spherical particles and shorter growth times but in the 3-day particles there are quite a few cube shaped particles. It is possible that even though the particles get larger with larger growth time that the intercrystalline gaps can get smaller due to the different particle geometries. This would support the fact that a densification process is occurring during longer reaction times.

Table 2 also shows the total and mesoporous BET surface area in m^2/g for the various silicalite powders. The total BET surface area is very similar for the different powders. The mesoporous surface area increases with increasing growth time. The fact that the mespopore area in Table 2 is increasing with increasing synthesis time does not support densification, but this increase in mesopore size may be attributed to adsorption at much higher P/P_0 values.

Supported silicalite membranes were prepared by dip coating the silicalite sol onto the α-alumina supports with the use of a hydroxypropyl cellulose binder. The membranes were prepared from the 0.5-day sol unless otherwise specified. Figure 7 shows the cross section of the silicalite layer on the α-alumina support for membranes that were dip-coated with 1 wt% silicalite and 4 wt% silicalite sols. These membranes were dip-coated once and they were calcined at 650 °C. The one time dip-coated 1 wt% silicalite membranes were pinhole free, as verified by SEM observation. Coated silicalite layers thinner than 1 μm were found discontinuous on the alumina support. Two-time dip-coated membranes were made from the 1 wt% silicalite dip-coating solutions and were found to have a thickness of about 6 μm. These membranes were calcined between the 1st and 2nd dip-coating. One-time dip-coated membrane made from 4 wt% silicalite sol gave a silicalite membrane of about 12 μm

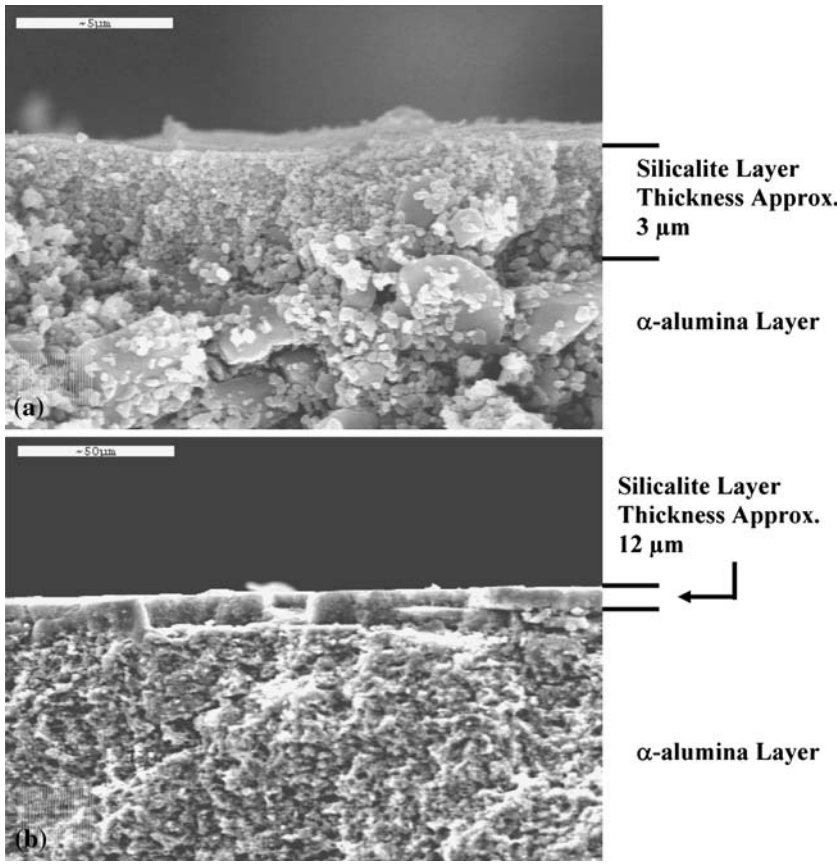

Fig. 7 SEM of cross section of a silicalite membrane on an α-alumina support. (**a**) 1 time dip-coated with 1 wt% silicalite, 5 μm scale bar, (**b**) 1 time dip-coated with 4 wt% silicalite, 50 μm scale bar

in thickness. The thickness of the membranes was confirmed by measuring the silicon profile with SEM/EDS. Through the use of SEM/EDS it was also determined that the silicalite zeolite does not penetrate more than 1.0 μm into the surface of the alumina support. Figure 8 shows XRD patterns of these three supported silicalite membranes and that for the alumina support. As shown, the intensity of the XRD peaks for silicalite related to those for alumina support increases with increasing thickness of the silicalite membrane. Supported silicalite membranes of various thicknesses can be prepared by controlling dip-coating times and the solid concentration of the silicalite sol. The membranes in this work were made thick for better XRD analysis.

Figure 9 shows the XRD patterns for silicalite powder that have been grown hydrothermally for 1 day, at the top of the chart, and a 12 μm thick silicalite membrane supported on α-alumia, on the bottom of the chart. The 12 μm thick silicalite membrane, which was made from a 4 wt% silicalite dip-coating solution, was chosen for comparison because it has the most pronounced silicalite peaks. Both the powder and the membrane have been calcined at 650 °C. It is apparent that the XRD peaks from silicalite are very similar in the two patterns, differing only in intensity. From the XRD patterns it can be concluded that the crystals on the membrane surface are randomly oriented, as would be expected from the dip-coating synthesis method used.

Single gas helium permeation experiments were conducted to see how the He gas permeation would be affected by the addition of the silicalite layers to the α-alumina support. Figure 10 shows the He permeance versus the average pressure for the same membrane at different stages of modification. The top curve shows that the permeance of the α-alumina support alone

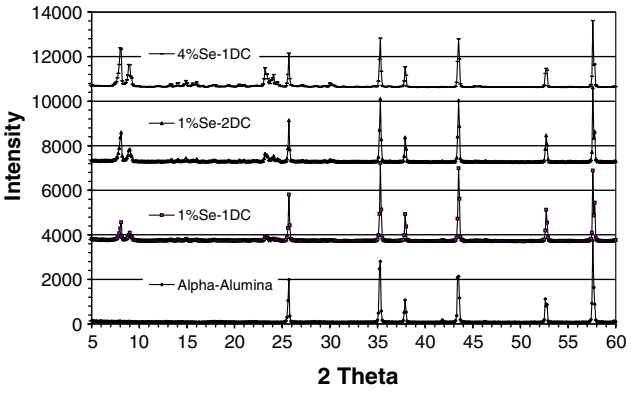

Fig. 8 XRD response of α-alumina and silicalite membranes of varying thickness on α-alumina supports

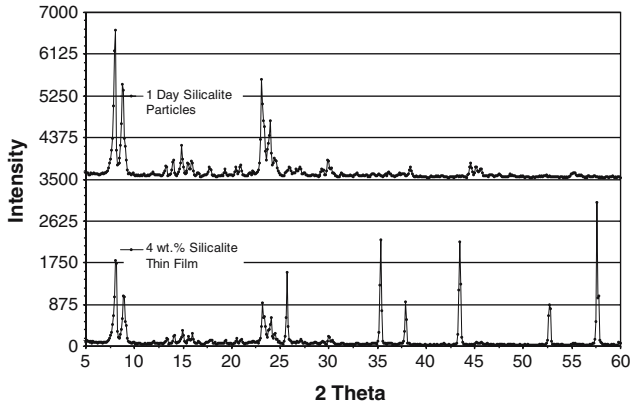

Fig. 9 XRD response of calcined silicalite powders made by hydrothermal synthesis lasting 1 day and of silicalite membrane on α-alumina support

ranged from 3.0×10^{-6} to 3.5×10^{-6} mol/m^2 s Pa. From this data it can be calculated that the average pore size of this support is approximately 190 nm [19]. The bottom curve shows that after one layer of silicalite (about 3 μm in thickness) is added the helium permeance is decreased by approximately 10%. The reduction in helium permeance by the 3 μm silicalite layer is smaller than the sol–gel derived mesoporous γ-alumina membrane of similar thickness [19] in spite of the similar mesopore sizes of these two membranes (3–4 nm as determined by nitrogen adsorption porosimetry on unsupported membranes). The difference in helium permeation between the mesoporous silicalite membrane and γ-alumina membrane is most likely that the former has micropores through which helium also permeates while the latter does not. The bimodal pore silicalite membranes offer less mass transport resistance as compared to other mesoporous membranes of similar pore size.

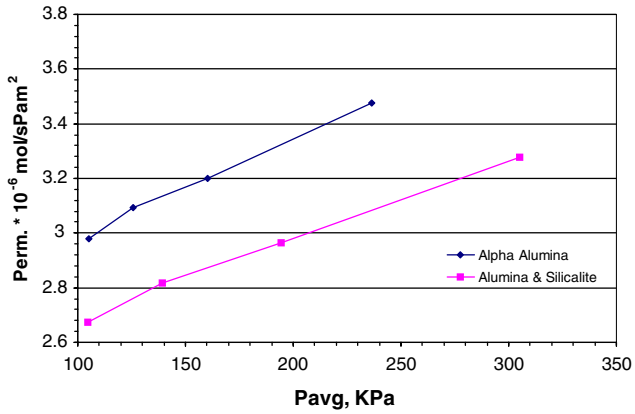

Fig. 10 Single gas helium permeation through unmodified α-alumina support and α-alumina support with 1 time dip-coated 1 wt% silicalite layer

It is possible that the relatively large He performance is due to cracks or pinholes. SEM and light microscopes were used and found the surface and cross section of the membranes to be defect free. The only way to truly determine the contribution of the micropores would be to do large molecule (SF_6) permeation experiments in addition to the He permeation experiments. Unfortunately these experiments could not be run.

Conclusions

Silicalite powders and supported silicalite membranes with a bimodal pore size distribution were made from silicalite particles that were grown for 0.5, 1, 2, and 3 days. From visual inspection of SEM pictures the average particle diameters of the silicalite particles were 150, 220, 300, and 380 nm for the 0.5-, 1-, 2-, and 3-day particles, respectively. For the silicalite powders the mesopore size decreases and mesopore surface area increases with increasing silicalite agglomerate size as a result of a change of the shape of silicalite agglomerates from round to more faceted one. Continuous supported silicalite thin films of thicknesses ranging from 3 μm to 12 μm were made by the sol–gel dip-coating of the silicalite sols on alumina support. The thickness of the coated silicalite layer can be readily controlled by varying the dip-coating times or sol concentration. Single gas He permeance of the 3 μm α-alumina supported silicalite membrane was found to be from 2.7×10^{-6} to 3.3×10^{-6} mol/m^2 s Pa in the range of pressures used.

Acknowledgement We are grateful to Department of Army through a MURI grant for providing the financial support for this work.

References

1. Weitkamp J (2000) Solid State Ionics 133:175
2. Yang Z, Lin YS (2000) Ind Eng Chem Res 39:4944
3. Lovallo M, Tsapatsis M (1996) Chem Mat 8:1579
4. Lin YS, Kumakiri I, Nair BN, Alsyouri H (2002) Separ Purif Methods 32:229
5. Pan M, Lin YS (2001) Micro Meso Mat 43:319
6. Yuan W, Lin YS, Yang WS (2004) J Am Chem Soc 126:4776
7. Moos R, Muller R, Plog C, Knezevic A, Leye H, Irion E, Braun T, Marquardt KJ, Binder K (2002) Sen Act B Chem 83(1–3):181
8. Sasaki I, Tsuchiya H, Nishioka M, Sadakata M, Okubo T (2002) Sen Act B Chem 86(1):26
9. Cooper CA, Lin YS, Gonzalez M (2004) J Memb Sci 229:11
10. Hedlund J, Noack M, Kolsch P, Creaser D, Caro J, Stert J (1999) J Memb Sci 159:263
11. Zhang YH, Chen F, Shan W, Zhang JH, Dong AG, Cai WB, Yang Y (2003) Micropor Mesopor Mater 62:277
12. Dong J, Wegner K, Lin YS (1998) J Memb Sci 148:233
13. Raileanu M, Popa M, Moreno JMC, Stanciu L, Bordeianu L, Zaharescu M (2002) J Memb Sci 210:197
14. Valtchev V (2002) J Mater Chem 12:1914
15. Naik SP, Chen JC, Chiang AST (2002) Micropor Mesopor Mater 54:293
16. Takata Y, Toshinori T, Yoshioka T, Asaeda M (2002) Micropor Mesopor Mater 54:257
17. Vroon ZAEP, Keizer K, Gilde MJ, Verweij H, Burggraaf AJ (1996) J Memb Sci 113:293
18. Burggraaf AJ, Vroon ZAEP, Keizer K, Verweij H (1998) J Memb Sci 144:77
19. Lin YS, Burggraaf AJ (1993) J Memb Sci 79:65